A New Dynamical Formulation for the UK Meteorological Office Unified Model

T Davies, M J P Cullen, M H Mawson and A J Malcolm

Meteorological Office

Bracknell, UK

1 Introduction

Modelling systems such as the Unified Model (UM) at the UK Meteorological Office or the ECMWF IFS (Integrated Forecast System) represent a considerable investment (many tens of person-years!) therefore upgrading the model by making major changes needs justification. An idea of the range of choices may be obtained from reading *Numerical Methods in Atmosphere and Ocean Modelling. The Andre Robert Memorial Volume. Editors C.Lin, R.Laprise, H.Ritchie* (1997), an excellent volume of current research issues in NWP.

This paper will only briefly discuss some of these choices but several other talks in these seminars will go into more detail; in particular Piotr Smolarkiewicz on time differencing and nonhydrostatic modelling, Andrew Staniforth on semi-Lagrangian methods and Aidan McDonald on physics coupling. The design of the scheme is based largely on earlier work done by Mike Cullen in the context of balanced models and he will discuss these issues in his talk.

In the next section we discuss a range of choices for the dynamics of NWP and climate models. This is followed by an outline of semi-implicit, semi-Lagrangian schemes and coupling with physics parametrizations. In section 5 we present an outline of the actual scheme proposed for the new dynamics of the UM followed by brief details regarding parallelisation of the code. In section 7 we discuss testing of the scheme in a set of tests ranging from idealised dynamics-only tests to full model climate and forecast tests.

2 New Dynamics Choices

There are many choices to make in building a model for NWP or climate modelling. There are many choices for the dynamics alone and the list shown in table 1 compares the choices made for the UM , the ECMWF model and a proposed new formulation for the

MODEL	Unified Model	ECMWF	New Dynamics
EQUATIONS	Hydrostatic Pseudo-radius 3D-Coriolis	Hydrostatic Shallow atmosphere Vertical Coriolis	non-Hydrostatic Height based 3D-Coriolis
HORIZONTAL GRID	Regular latitude-longitude	Reduced Gaussian grid	Regular latitude-longitude
HORIZONTAL STAGGERING	B-grid	Spectral T_L213	C-grid
HORIZONTAL RESOLUTION	432*325	640*320	432*325
VERTICAL COORDINATE	Hybrid	Hybrid	Hybrid
	sigma-pressure	sigma-pressure	Height
VERTICAL STAGGERING	Lorenz	Lorenz	Charney-Phillips
VERTICAL RESOLUTION	30 levels	31 levels	38 levels
TIME-SCHEME	Split-explicit 2 time-level	Semi-implicit 2 time-level	Semi-implicit 2 time-level
TIME-STEP	Physics 1200secs Dynamics 400secs	Physics 20mins Dynamics 20mins	Physics 30mins Dynamics 30mins
ADJUSTMENT SCHEME	Forward-backward Basic state profile	Semi-implicit Spectral Basic state profile	Semi-implicit Pressure correction NO Basic state profile
SOLVER	None	Spectral 2d Helmholtz equation	GCR(k) 3d Helmholtz equation
ADVECTION SCHEME	Explicit Heun	Semi-Lagrangian Horizontal quasi-monotone 3d q	Semi-Lagrangian Horizontal quasi-monotone 3d q
CONSERVATION	Angular momentum Mass First moments	Angular momentum	Angular momentum Mass
DIFFUSION	del2(Kdel2) Conservative, local	Kdel4	None
DAMPING/FILTERING	Fourier filtering Time-filter on winds	Decentring Time-filter	Decentring

Table 1: Model Comparison

dynamics of the UM. Some of these choices can be changed quite easily within an existing model but others require either a complete re-writing of the model code or at least major reconstruction.

There are several shortcomings in the UM dynamics which need addressing.

1. A large moist bias at low vertical resolutions.
2. Significant time-truncation errors and time-step dependencies.
3. Noise problems and the need for excessive artificial diffusion.
4. Inadequate coupling between dynamics and physics.
5. Inadequate coupling between dynamics and data assimilation.
6. Flow across the poles.

The above problems can be addressed by tackling the following issues.

1. Using a more accurate advection scheme, especially in the vertical where the current scheme contributes to an excessive moist bias at low vertical resolutions.
2. Improving the model balance to minimize noise problems, to reduce the requirement for excessive artificial diffusion and to control vertical transports.
3. Improving the model balance to give better coupling with the data assimilation and with the physics.
4. Use schemes that avoid or reduce problems with flow across the poles.

Experience elsewhere suggests using semi-Lagrangian advection would meet the requirements for 1. above but this cannot be used with the split-explicit scheme without incurring time-splitting errors and alternatives (viz. positive definite advection scheme) have not been made to work adequately. Using semi-Lagrangian advection cost-effectively requires using a semi-implicit time-scheme and changing to a C-grid staggering in the horizontal. This would also improve the balance of the model and addressing 2, 3 and 4 above. These changes alone would result in major changes to the UM and lead on to significant re-tuning and upgrading of the physics. Item 3 above can also be addressed by changing the vertical staggering from the Lorenz staggering to a Charney-Phillips staggering. This adds to the reorganisation of the code and introduces some problems in interfacing with the physics. Further improvements can be obtained by changing the solution procedure,

in particular using the full temperature profile in the pressure gradient term rather than splitting into a basic-state and residual but at the cost of having to use a more-expensive, three-dimensional solver. This allows better treatment of dynamics-physics coupling which will be discussed in Mike Cullen's paper in these proceedings. It also allows the model to be non-hydrostatic and be run at very-high resolution (1-2km or less). The current mesoscale model version of the UM is unlikely to be adequate at resolutions higher than 5km and there is evidence of noise problems near orography at slightly higher resolutions than the current 15km or so.

3 Semi-Implicit Semi-Lagrangian Schemes

Consider an advection equation for a variable X representing either u, v, w, θ (or T) q (or other moisture variables)

$$\frac{\mathrm{D}X(\mathbf{x},t)}{\mathrm{D}t} = D(\mathbf{x},t) + P(\mathbf{x},t) \tag{1}$$

where $D(\mathbf{x},t)$ contains dynamics forcing terms and $P(\mathbf{x},t)$ contains physics forcing terms.

A typical semi-implicit, semi-Lagrangian (SISL) formulation for this equation is,

$$\begin{aligned} X^{n+1} = X_d^n \quad &+ \quad \Delta t[(1-\alpha_D)D_d(\mathbf{x}_d,t^n) + \alpha_D D(\mathbf{x},t^{D*})] \\ &+ \quad \Delta t[(1-\alpha_P)P_d(\mathbf{x}_d,t^n) + \alpha_P P(\mathbf{x},t^{P*})] \end{aligned} \tag{2}$$

where subscript $_d$ refers to the departure point of the trajectories. Values at the departure points have to be interpolated from information at gridpoints. Further information on semi-Lagrangian schemes may be found in Andrew Staniforth's contribution to these proceedings. The α's are the implicit weightings. $\alpha = 0$ for explicit updating and $\alpha = 1$ with $t^* = t^{n+1}$ for fully implicit updating. Ideally $\alpha = \frac{1}{2}$ in semi-implicit schemes but often α needs to be a little larger than $\frac{1}{2}$ to damp the scheme. Using $t^* = t^{n+1}$ is only practicable if either we can evaluate the terms $D(t^{n+1})$ and $P(t^{n+1})$ without knowledge of $X(t^{n+1})$ or that we can obtain an expression of the form $\mathbf{Q}(\mathbf{x},t)X^{n+1}$ which then can be put on the *LHS* and used to evaluate X^{n+1} provided $[\mathbf{I} - \mathbf{Q}(\mathbf{x},t)] \neq \mathbf{0}$. It is typical practice in NWP to linearise the pressure gradient term around a basic state temperature profile which enables $\mathbf{Q}_{ref}(\mathbf{x})X^{n+1}$ to be placed on the *LHS*. This also allows the system to decouple into a set of two-dimensional equations which can be solved efficiently either by using direct methods such as a spectral technique or by using other efficient methods such as multigrid techniques. However, the physics terms cannot be vertically decoupled

so that these normally remain as *RHS* forcing terms along with the remaining part of the linearised pressure gradient terms.

4 Physics Coupling

There are basically two choices as to where to call the parametrizations, either after the adjustment or after the advection, i.e. we can order (adjustment, advection, physics) or (adjustment, physics, advection). In addition there are choices as to which time-level to increment since for example, the advection and physics could be process-split and both use the fields from the adjustment as input or the physics could be fractionally stepped with the output from one process passed onto the next process. In the latter situation, changing the ordering of the physics will change the results whereas if the physics are totally process split then the ordering does not matter.

The physical processes have a range of timescales. It is usual to think of processes as being either fast or slow. Ordering of processes from slowest to fastest might be radiation, hydrology, convection, convective momentum transport, gravity-wave drag, boundary layer, cloud, large-scale precipitation. If these are process-split then the ordering is irrelevant. However, the faster processes may need to know about changes (tendencies) if a long physics timestep is used. The structures themselves should be calculated from a balanced or equilibrium state (i.e. realistic states) but redistribution needs to know what forcing is taking place. On the other hand, slow processes should properly be calculated from a balanced or equilibrium state as this is nearer to reality. In the dynamics the advection is a slow process whilst the adjustment is fast and needs to know how much destabilisiation is produced by the advection (e.g. the rate of destruction of thermal wind balance by the (geostrophic) flow). Aidan McDonald discusses these issues in his paper.

4.1 Physics Coupling with SISL schemes

Consider just the physics updating in the equations of the previous section.

$$X^{n+1} = X_d^n + \Delta t[(1-\alpha_P)P_d(\mathbf{x}_d, t^n) + \alpha_P P(\mathbf{x}, t^{P*})] \tag{3}$$

where the $P's$ are the sum of the physics processes. As explained above, $t^{P*} = t^{n+1}$ is only practicable if we can obtain an expression of the form $\mathbf{Q}(\mathbf{x}, t)X^{n+1}$ which can then be put on the *LHS* and included in the solver step. This could be done for the boundary

layer which can be written as

$$K(t^{P*})V(\theta(t^{P*})) = K(t^n)V(\theta(t^{P*})) = K(t^n)V(\theta(t^n) + \gamma\theta') \tag{4}$$

where K are the diffusion coefficients, V is a vertical operator and γ are the boundary layer implicit weights. This form of boundary layer treatment follows that indicated in section 7.2 of Cullen (1997) but as yet we have not managed to include these terms successfully in our formulation. In the new dynamics we use $\alpha_P = 0$ for all the physical processes except for the boundary layer and convection where we use $\alpha_P = 1$. The time level for the boundary layer is described in section 5.3 below. For convection we use the partially updated fields as input since we require the convection to remove instability produced by the other processes.

5 Outline of New Dynamics Scheme

5.1 Dynamics

The main features of the new dynamics scheme are:

- Non-hydrostatic equations with height as vertical coordinate.
- Charney-Phillips grid staggering vertically, i.e. potential temperature on same levels as vertical velocity including top and bottom boundaries where vertical velocity is zero.
- C-grid staggering horizontally, i.e. u-component east-west staggered from temperatures and v-component north-south staggered from temperatures.
- Vector semi-Lagrangian advection scheme.
- Semi-implicit time-scheme without the removal of a basic state profile and with an appropriate solver for a variable coefficient problem.

The procedure used for solving the equations is a predictor-corrector method similar to that used by Cullen (1989). Initial estimates of the wind components, potential temperature and humidity variables are obtained by semi-Lagrangian advection using the two time-level scheme of Bates et al (1993). Only current time-level information is used in the right-hand side terms. These estimates are used to construct a set of correction equations. To obtain a correction equation for the (3-dimensional) pressure we require that

the equation of state is satisfied at the new time-level. and we linearise the equation of state with respect to the differences between the time-levels. We manipulate these correction equations to obtain a 3-dimensional variable coefficient Helmholtz-type equation for the (Exner) pressure correction. Once the pressure correction is known we can then derive the corrections and hence the new time-level values for the other variables. The physics parametrizations are called before the correction step so that the dynamics and physics increments are used in calculating the balanced state at the new time-level. A fuller description of the scheme is in Cullen et al (1998).

5.2 Physics Parametrizations

The physics package used by the new dynamics consists of :-

- Edwards-Slingo radiation scheme with non-spherical ice spectral files (Edwards and Slingo, 1996)
- Large-scale precipitation with new prognostic ice microphysics.
- Vertical gradient area large-scale cloud scheme.
- Convection with options for CAPE closure, momentum transports and convective anvils.
- New (non-local in unstable regimes) boundary-layer scheme.
- Gravity-wave drag.
- MOSES (Met. Office Surface Exchange Scheme) surface hydrology and soil model scheme.

These parametrizations have been developed for the latest climate model version of the UM to be used for climate change experiments at the UK Meteorological Office. Within the set of parametrizations above there are many parameters that need to be set. For example, there are options which directly affect the clouds in the model such as the critical relative humidities and the convective anvils. The various options have been chosen by experiment and using the experience gained in developing the latest climate model version of the UM.

5.3 Momentum Equation

The momentum equation for u can be written as

$$\frac{Du}{Dt} = fv - \frac{1}{\rho}\frac{\partial p}{\partial x} + P + \mathbf{F}(\underline{u}) \tag{5}$$

where P is the physics forcing excluding the boundary layer scheme, $\mathbf{F}$ is a matrix of boundary layer coefficients calculated from some given input data applied to the vertical column of u values denoted $\underline{u}$. The semi-implicit semi-Lagrangian version of this is

$$\begin{aligned} u^{n+1} &= u_d^n \\ &- \Delta t(1-\alpha_{pg})\left[\frac{1}{\rho}\frac{\partial p}{\partial x}\right]_d^n - \Delta t\alpha_{pg}\left[\frac{1}{\rho}\frac{\partial p}{\partial x}\right]^{n+1} \\ &+ \Delta t(1-\alpha_c)\left[fv\right]_d^n + \Delta t\alpha_c\left[fv\right]^{n+1} \\ &+ \Delta t(1-\alpha_p)P_d^n + \Delta t\alpha_p P^{n+1} \\ &+ \Delta t(1-\alpha_f)\left[\mathbf{F}(\underline{u})\right]_d^n + \Delta t\alpha_f\left[\mathbf{F}(\underline{u})\right]^{n+1} \end{aligned} \tag{6}$$

where the α's are time-weights, and subscript d denotes values at the semi-Lagrangian departure points, superscripts n and $n+1$ denote values at the old and new time-levels respectively. For stability it is required that $\alpha_{pg} \geq 0.5$ and $\alpha_f \geq 0.5$. In the process split new dynamics $\alpha_p = 0$ except for convection (which provide convective momentum transport terms for u) where $\alpha_p = 1$.

We choose $\alpha_f = 1$ and this gives the following boundary layer term in equation (6)

$$\Delta t\left[\mathbf{F}(\underline{u})\right]^{n+1} \tag{7}$$

This is simplified by calculating the matrix of coefficients $\mathbf{F}$ purely from time-level n data so that we replace equation (7) with

$$\Delta t\left[\mathbf{F}^n(\underline{u}^{n+1})\right] \tag{8}$$

Equation (6) becomes

$$\begin{aligned} u^{n+1} &= u_d^n \\ &- \Delta t(1-\alpha_{pg})\left[\frac{1}{\rho}\frac{\partial p}{\partial x}\right]_d^n - \Delta t\alpha_{pg}\left[\frac{1}{\rho}\frac{\partial p}{\partial x}\right]^{n+1} \end{aligned} \tag{9}$$

$$
\begin{aligned}
&+ \Delta t(1-\alpha_c)\,[fv]_d^n + \Delta t\alpha_c\,[fv]^{n+1} \\
&+ \Delta t P_d^n \\
&+ \Delta t\left[\mathbf{F}^n(\underline{u}^{n+1})\right]
\end{aligned}
$$

The best solution procedure would be to solve equation (9) as it stands. This is complicated by the need to substitute this equation into the similar equation for v so that u^{n+1} and v^{n+1} can be obtained in terms of p^{n+1} for the semi-implicit solver step. This substitution is currently considered to be too complicated and expensive to perform. Therefore a cheaper, simpler solution is required.

5.3.1 Solution of equation (9)

Let $u' = u^{n+1} - u^n$, $p' = p^{n+1} - p^n$, etc, then equation (9) can be written as

$$
\begin{aligned}
u^{n+1} &= u_d^n \\
&- \Delta t(1-\alpha_{pg})\left[\frac{1}{\rho}\frac{\partial p}{\partial x}\right]_d^n - \Delta t\alpha_{pg}\left[\frac{1}{\rho}\frac{\partial p}{\partial x}\right]^n - \Delta t\alpha_{pg}\left[\frac{1}{\rho}\frac{\partial p'}{\partial x}\right] \\
&+ \Delta t(1-\alpha_c)\,[fv]_d^n + \Delta t\alpha_c\,[fv]^n + \Delta t\alpha_f\,[fv'] \\
&+ \Delta t P_d^n \\
&+ \Delta t\left[\mathbf{F}^n(\underline{u}^{n+1})\right]
\end{aligned}
\tag{10}
$$

where ρ^{n+1} has been replaced by ρ^n in the pressure gradient term. The solution of equation (10) is now split into several steps.

Step 1:

Calculate R_u, the explicit increment to u which uses semi-Lagrangian advection, given by

$$
\begin{aligned}
R_u &= u_d^n \\
&- \Delta t(1-\alpha_{pg})\left[\frac{1}{\rho}\frac{\partial p}{\partial x}\right]_d^n - \Delta t\alpha_{pg}\left[\frac{1}{\rho}\frac{\partial p}{\partial x}\right]^n \\
&+ \Delta t(1-\alpha_c)\,[fv]_d^n + \Delta t\alpha_c\,[fv]^n \\
&+ \Delta t P_d^n \\
&- u^n
\end{aligned}
\tag{11}
$$

Step 2:

Solve the Boundary Layer implicit equation

$$
u^* - (u^n + R_u) = \Delta t\mathbf{F}^n(\underline{u}^*) \tag{12}
$$

Step 3:

Solve the semi-implicit step

$$\begin{aligned} u^{n+1} &= u^* \\ &- \Delta t \alpha_{pg} \left[\frac{1}{\rho} \frac{\partial p'}{\partial x} \right] \\ &+ \Delta t \alpha_c \left[f v' \right] \end{aligned} \tag{13}$$

Similar equations are obtained for v^{n+1}, w^{n+1} and θ^{n+1}. ρ^{n+1} is obtained using an Eulerian treatment of the continuity equation. We then require that the equation of state be satisfied at time $n+1$. Substituting $p^{n+1} = p^n + p'$, $\theta^{n+1} = \theta^n + \theta'$, $\rho^{n+1} = \rho^n + \rho'$ and linearising the equation of state gives an expression for p', θ' and ρ' in terms of time level n values. We have six equations for the six corrections which can be reduced to one Helmholtz-type equation for the pressure correction p'. Solving this equation for the pressure correction, we can then back substitute to find the corrections for the other variables.

5.4 Solver

For the Helmholtz equation we use a generalised conjugate residual (GCR) method described by Smolarkiewicz and Margolin (1994). In common with other iterative conjugate gradient techniques, preconditioning is usually required to achieve convergence within a reasonable number of iterations. A vertical preconditioning is adequate for uniform horizontal resolution. In global configurations further preconditioning is required since the convergence of the meridians of the latitude-longitude grid results in the east-west gridlength becoming much smaller than the north-south gridlength which in turn leads to an increase in iterations of the solver. We use an ADI (alternating direction implicit) preconditioning step in the iteration as proposed by Skamarock et al (1996). We use the ADI preconditioner in the longitudinal and vertical directions since these directions possess most of the variation in the pressure correction. At N216 (432 points east-west) near the poles the v-components are less than a kilometre apart in the longitude direction compared with 60km apart at mid-latitudes. The ADI preconditioner is cost-effective even at N48 (96 points east-west) resolution used for climate modelling, i.e. the iteration count is reduced sufficiently to offset the overhead of performing the ADI steps.

At N216 the ADI preconditioner results in a reduction of around two thirds in the iteration count than by using the vertical preconditioner alone. However, the large variation

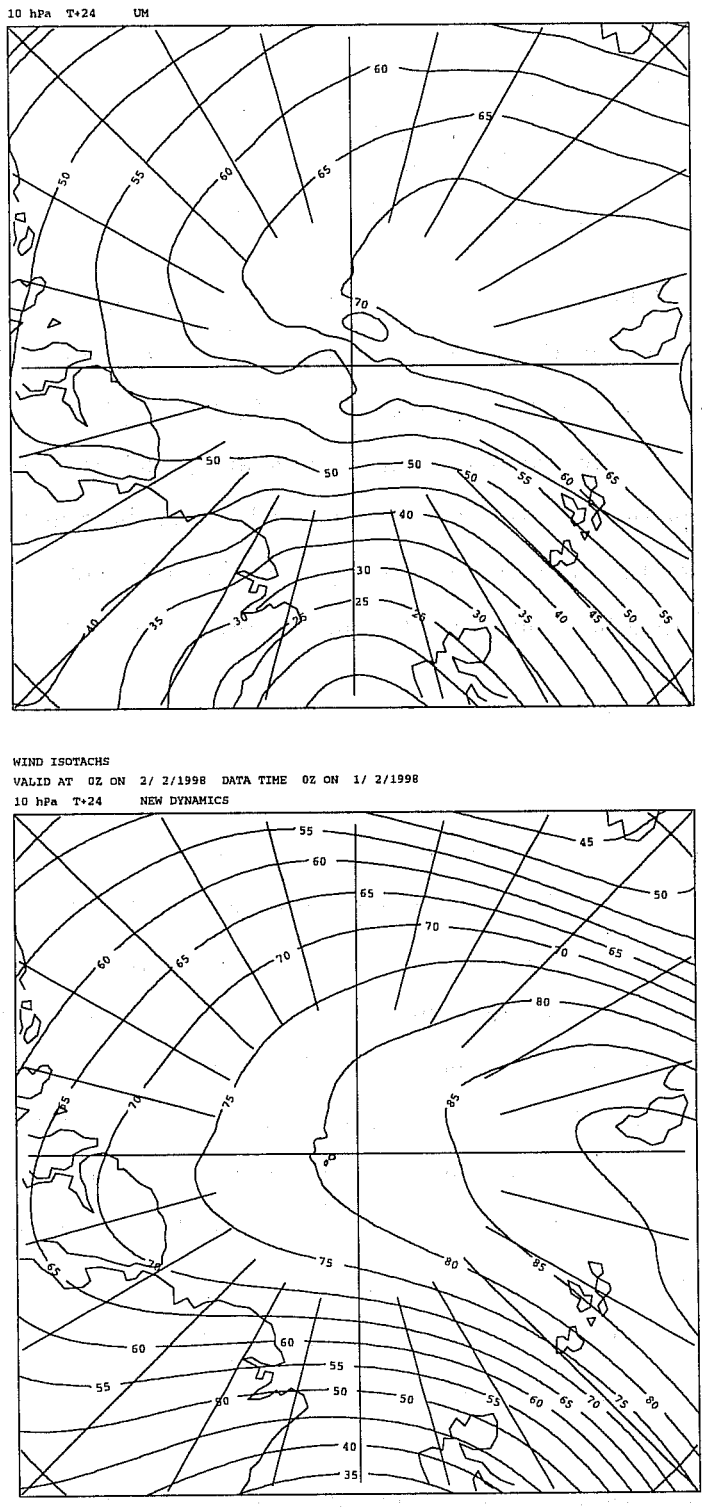

Figure 1: Isotachs (5m/s contours) of 10hPa wind for T+24 forecast valid at 00UTC 2/2/98. Upper panel from UM. Lower panel from new dynamics.

near the poles still results in too many iterations being required to converge the solution in these regions. We therefore use a filter on the orography fields and use multiple applications of simple 1-2-1 filters to remove the very short wavelengths from the winds and temperatures. This has proved to be successful in reducing the iteration count to acceptable levels. Even with the use of the filter, cross-polar flow in the new dynamics appears to be better handled than by the UM as can be seen by comparing T+24 forecasts of the 10hPa wind isotachs from both the UM and new dynamics (figure 1) for a case where there is a strong polar-night jet across the North Pole. In the UM the jet axis is not quite over the North Pole and over the Pole the winds are around 60 metres per second. The noise evident in the isotachs is due to the heavy filtering needed by the UM near the poles. In the new dynamics the jet axis is closer to the pole with winds in excess of 80 metres per second and only a small amount of noise is evident.

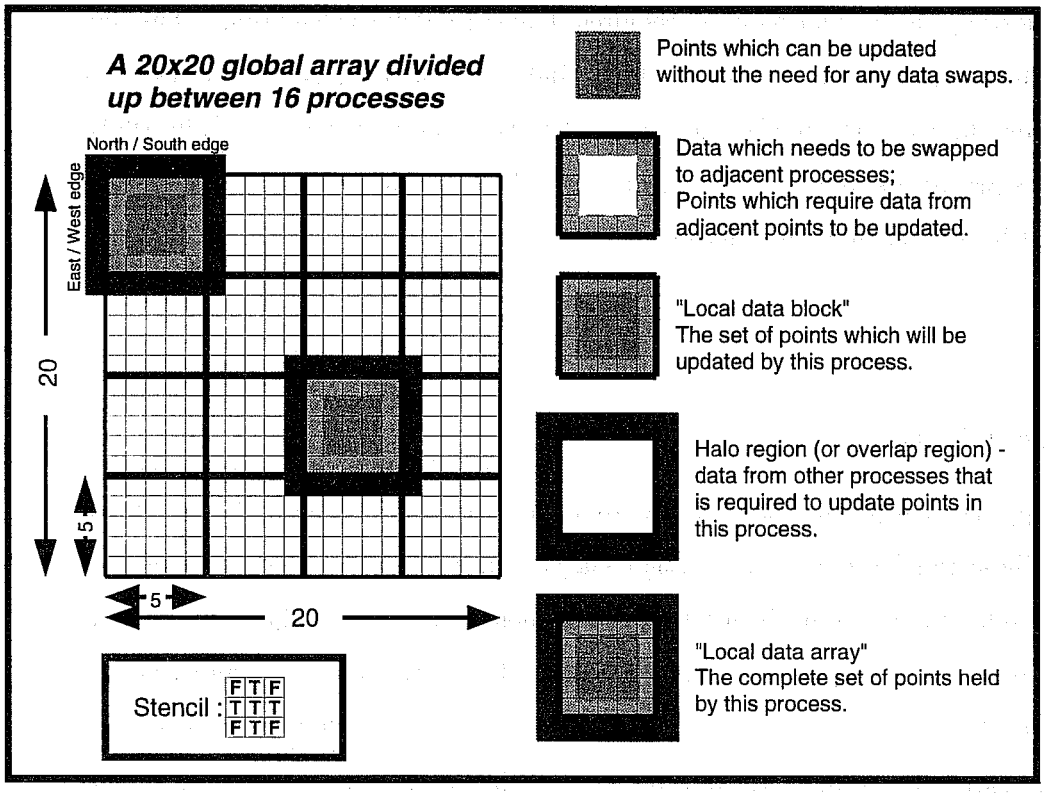

Figure 2: Regular Domain Decomposition

6 Parallelisation and Performance

Efficient parallelisation of the model code is essential in order to make best use of available computer power and to meet production schedules. An efficient parallelisation strategy

has been devised for the new dynamics which uses a similar (two-dimensional) domain decomposition as that of the UM (the full domain divided horizontally into blocks which each have the full number of levels) as shown in figure 2. The blocks may have a halo region of data from adjacent blocks which are required for some calculations such as differencing. If higher order differencing is used then the halo can be increased. At various times during the timestepping, data needs to be swapped between processors to update the haloes. It is important that the decomposition results in a sharing out of the work to achieve good load balance, otherwise processors may have to wait for one processor to complete its work.

For the semi-Lagrangian advection a 'communication-on-demand' approach is used. In this case the halo needs to be chosen depending on the Courant number and the order of the interpolations. In the east-west direction, where the Courant number may increase significantly as the poles are approached, for each departure point outside a processor boundary, the processor on which the point resides is identified and a message sent to each processor requesting the calculation of all required departure point calculations. The halo size is chosen to account for the maximum likely wind speed in the north-south direction. Timing tests on the complete model, including physics, show a speed-up of 3.95 (99%) from 72 to 288 processors and 6.5 (81%) from 72 to 576 processors thus demonstrating that the parallelisation strategy is efficient.

7 Tests

7.1 Idealised Tests

Idealised test problems provide a suitable environment for testing options and components of schemes. These can be done in the design stages and as a test of complete schemes. Exchanging results from test problems between modelling groups would be useful and instructive in assessing the performance and behaviour of various components and schemes. Some initiatives have been started, for example there is a set of shallow-water tests (see 7.3 below) and three-dimensional dynamical-core experiments (see 7.4 below) which have resulted in comparisons between some modelling groups.

7.2 Two-dimensional Idealised Tests

Before writing the new scheme the performance of the Charney-Phillips vertical staggering was evaluated on a set of three idealised problems in two-dimensions using a prototype

model. (see Cullen et al, 1997 for further details). The tests used were:

1. Density current.

2. Idealised Eady-wave simulations as in Nakamura and Held (1989).

3. A simulation of fog formation to test the problems of using a boundary-layer scheme. (Golding, 1993)

In the first test there was no difference between the two staggerings as expected. In the Eady-wave test the Charney-Phillips staggering developed less noise than the Lorenz staggering and was able to run through the initial front formation even without the use of artificial horizontal diffusion. The boundary layer test was used to resolve the problem of which quantities to average to calculate the mixing coefficients. The better strategy appears to be to average the potential temperature so that the exchange coefficients are calculated on the w/θ levels and then to average the mixing coefficient for heat and moisture, K_H.

Further two-dimensional xz tests have been carried out using the new dynamics scheme. The test problems considered so far are:

1. Density current (Straka et al 1993).

2. 2d flow over a hill, for both incompressible and compressible regimes.

3. Convective bubble tests (Robert 1993).

4. Steady flow over a cosine hill.

A sequence of results from the case of a large slightly warm bubble (plus 0.5K) and a small cold bubble (minus 0.1K) evolving in an isentropic atmosphere (300K) is shown in figure 3. This was run using a gridlength of 10 metres in both directions and with a 5 second timestep.

The convective bubble tests revealed two particular problems with our use of the scheme. One was due to a term which was believed to be small and omitted in the larger-scale tests. In this problem it proved necessary to include the term to achieve acceptable results. Secondly, the potential temperature advection needed to be made monotone but this particular choice does not work in our full atmospheric tests where potential temperature increases quickly at high altitudes. Similar problems were encountered in atmosphere

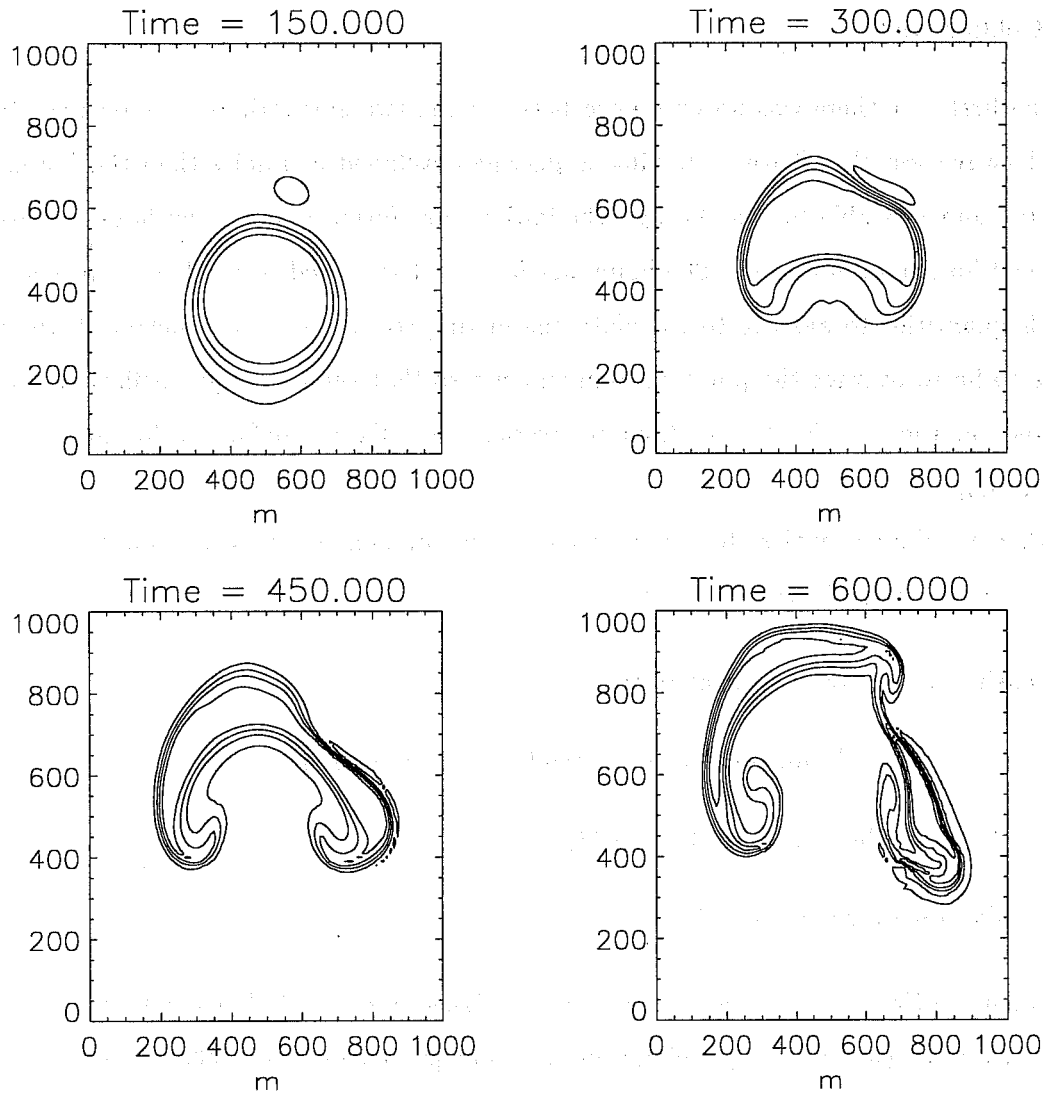

Figure 3: Evolution of a large warm bubble and small cold bubble in an isentropic atmosphere.

tests using a TVD (total variation diminishing, a first order monotone advection scheme) in the UM.

Results from the other test problems have shown acceptable performance and where comparisons can be made with results published elsewhere the results obtained so far are generally promising.

7.3 Shallow-Water Tests

Testing of the dynamics scheme on a set of seven shallow-water tests proposed by Williamson et al (1992) was completed. Acceptable results were obtained in all the tests Malcolm (1996). In particular, the improved performance of the semi-Lagrangian advection scheme over the UM scheme was demonstrated. In a real data height field test the new dynamics produced acceptable results with a 6 hour time-step at 96*65 global resolution. This compares with a 30 minute time-step used in the standard UM 96*73 climate configuration.

7.4 Three-dimensional Dynamics Tests

Full 3-d tests of the dynamics code on the dynamical core test as advocated by Held and Suarez (1994) have also been completed. This test is designed to try to compare different dynamical formulations without the complication of physics parametrizations. The model is run on a smooth planet with a simple surface friction and a prescribed temperature relaxation to produce an equator-pole temperature gradient and a realistic vertical structure. The model is then run for several hundred days when it reaches some equilibrium climate with baroclinic waves in mid-latitudes. Structures and energetics from different schemes and different resolutions can compared. Although there is no 'true' solution, comparisons between different schemes and resolutions are instructive. In particular, the test can reveal whether there is sensitivity of the tropical tropopause temperature due to the dynamics scheme. The new dynamics converges as vertical resolution is increased from 19 to 38 levels and above whereas the UM does not converge until the resolution exceeded 38 levels.

7.5 Climate Tests

AMIP (Atmospheric Model Intercomparison Project) climate tests using prescribed sea-surface temperatures have been used to evaluate the performance of the new dynamics as a climate model with resolution 96 points east-west, 73 points north-south and 38 levels in

(a) Zonal mean cross-section of temperature for djf
v26c08, 4 winters

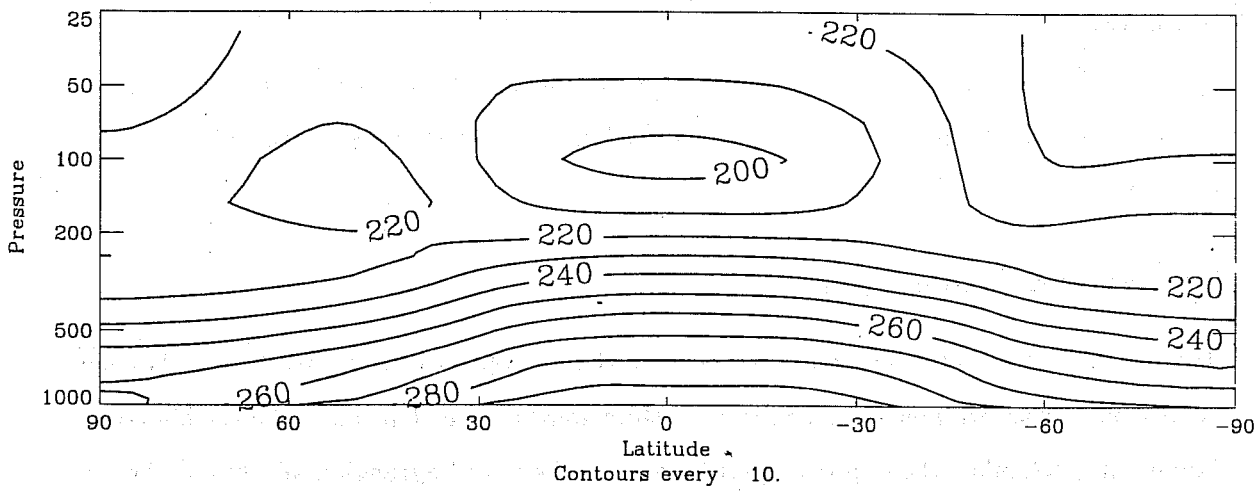

(b) Zonal mean cross-section of temperature for djf
v26c08, 4 winters minus HADAM4, 10 winters

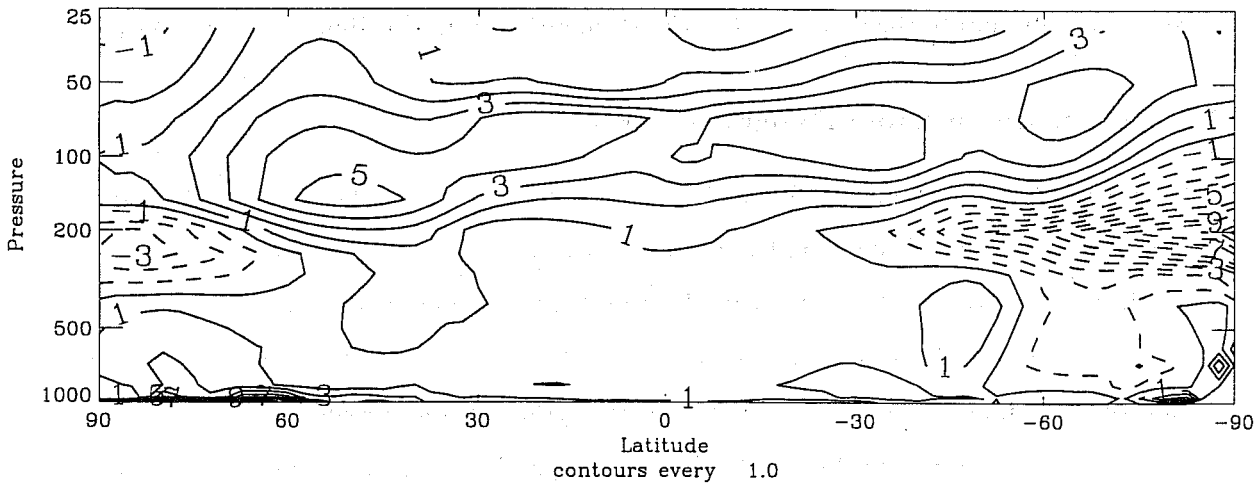

(c) Zonal mean cross-section of temperature for djf
v26c08, 4 winters minus ECMWF climatology 1979-88

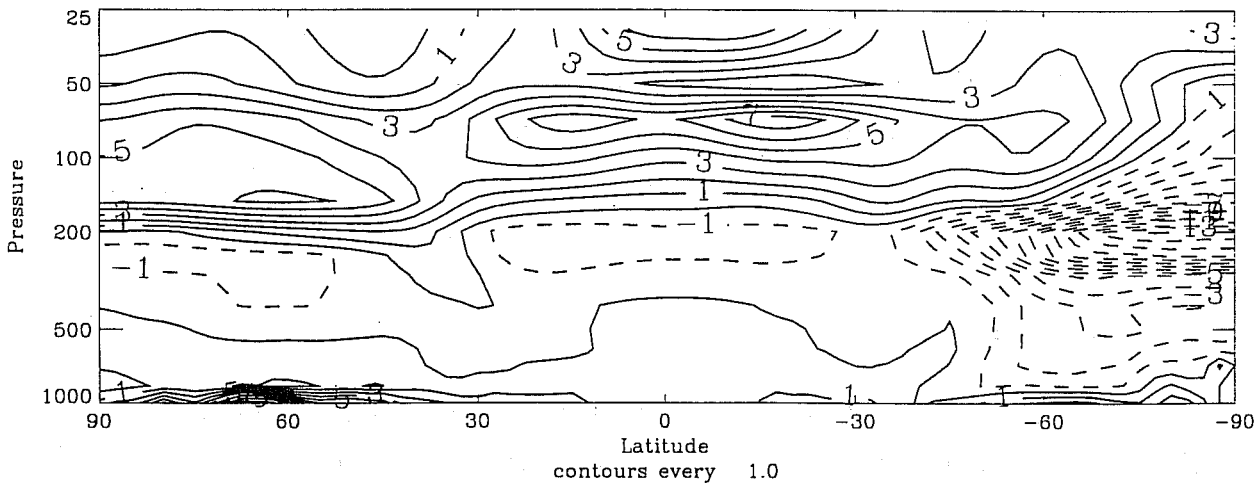

Figure 4: Climate comparison of zonal mean temperatures

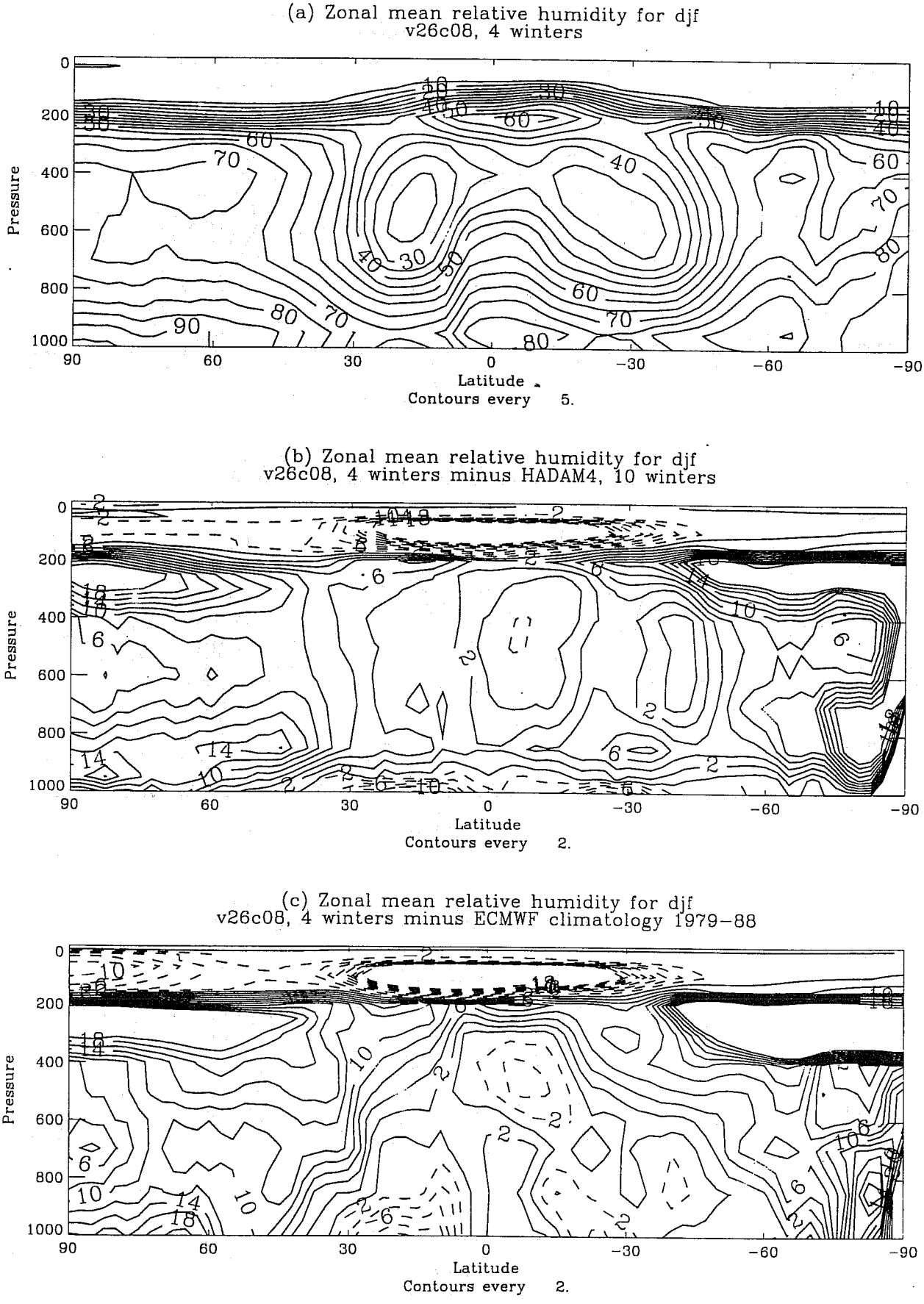

Figure 5: Climate comparison of zonal mean relative humidity

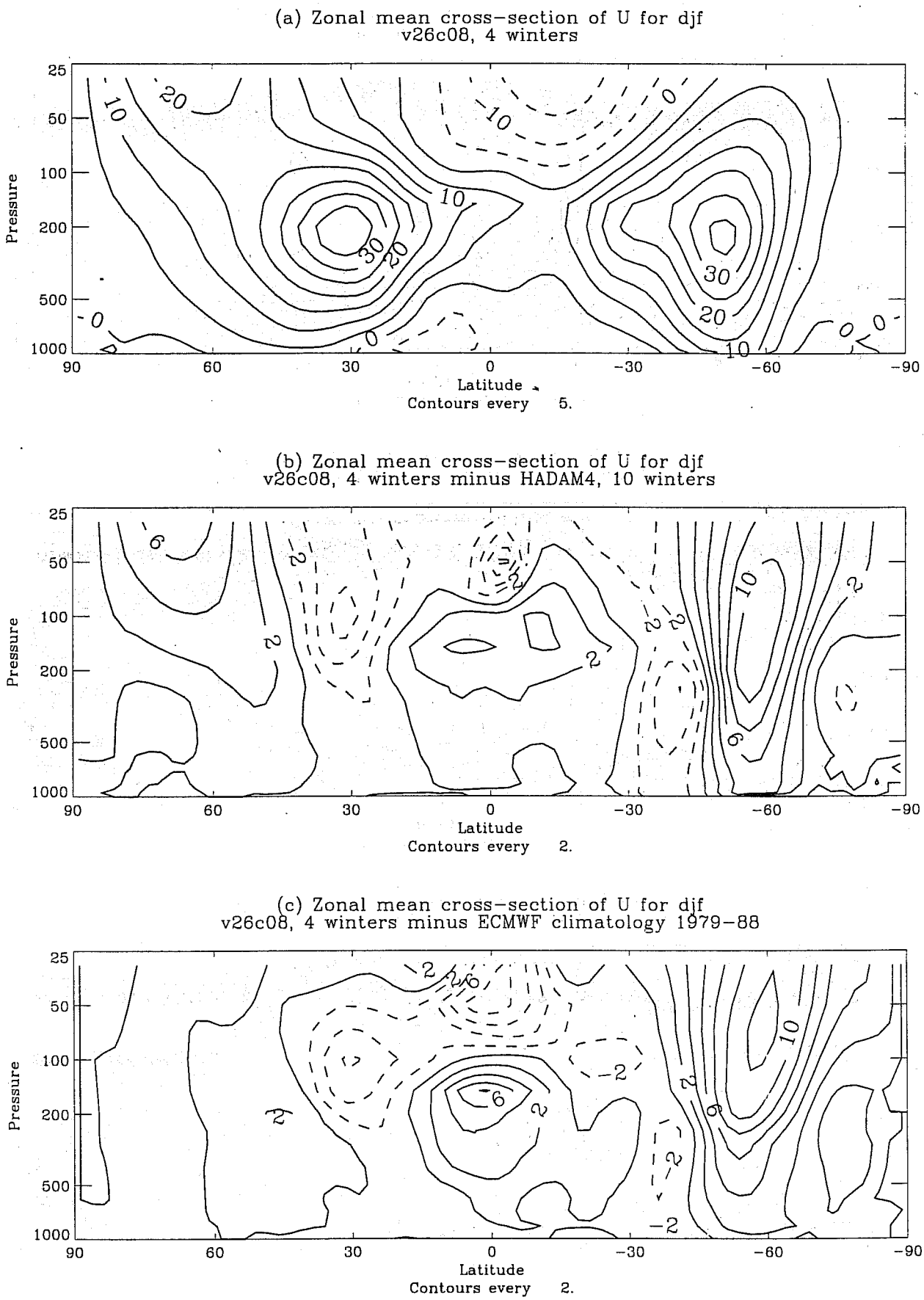

Figure 6: Climate comparison of zonal mean zonal wind

the vertical. An AMIP climate run usually consists of running from 1st December 1979 for a period of 10 years using prescribed sea-surface temperatures. Figures 4 to 6 show zonal mean plots of temperature, relative humidity and zonal wind respectively, from a four-winter average (December, January, February, djf) of a three year three month run of the new dynamics (top panel (a)), the difference from a ten-winter average of the UM climate model (middle panel (b)) and the difference from a ten-winter average of the ECMWF re-analysis climatology (lower panel (c)).

Tropical tropospheric temperature and humidity biases compare favourably with those from the latest UM climate model. However, in mid-latitudes the new dynamics is more moist and towards the poles is colder near the tropopause. These differences are known to be sensitive to differences in the details of the cloud schemes used in the two models. The position of the hydropause in the deep tropics is due partly to drying resulting from convection which is compensated by direct redistribution and horizontal diffusion in the UM, both processes which are not operating at present in the new dynamics.

The easterly bias above 200hPa near 30° North is due mainly to excessive drag over the Himalayas. The westerly bias in the southern hemisphere is mainly due to lack of drag partly since the orography has been smoothed and the Andes barrier height has been reduced and partly due to a lack of other drag mechanisms.

Many other features of the general circulation match the UM. Stratocumulus in the regions where there are extensive stratocumulus sheets (west of California, Peru and South West Africa) is much improved and 1.5m temperatures also appear to be improved because of improvements in low-level cloudiness. The apparent improvements in low-level cloudiness are thought to be due to the change in vertical staggering and perhaps to process splitting of the physics.

7.6 Operational Forecast Tests

A set of five day global forecast tests are being run using the latest physics settings as those used in the climate tests. Initial results were obtained using data interpolated from the UM operational model which is run with 432 points east-west, 325 points north-south and 30 levels in the vertical. The new dynamics uses the same horizontal grid resolution but has an extra 8 levels in the boundary layer.

Data has to be interpolated from the pressure-based hybrid coordinate system of the UM to the height-based hybrid coordinate used in the new dynamics. This means that

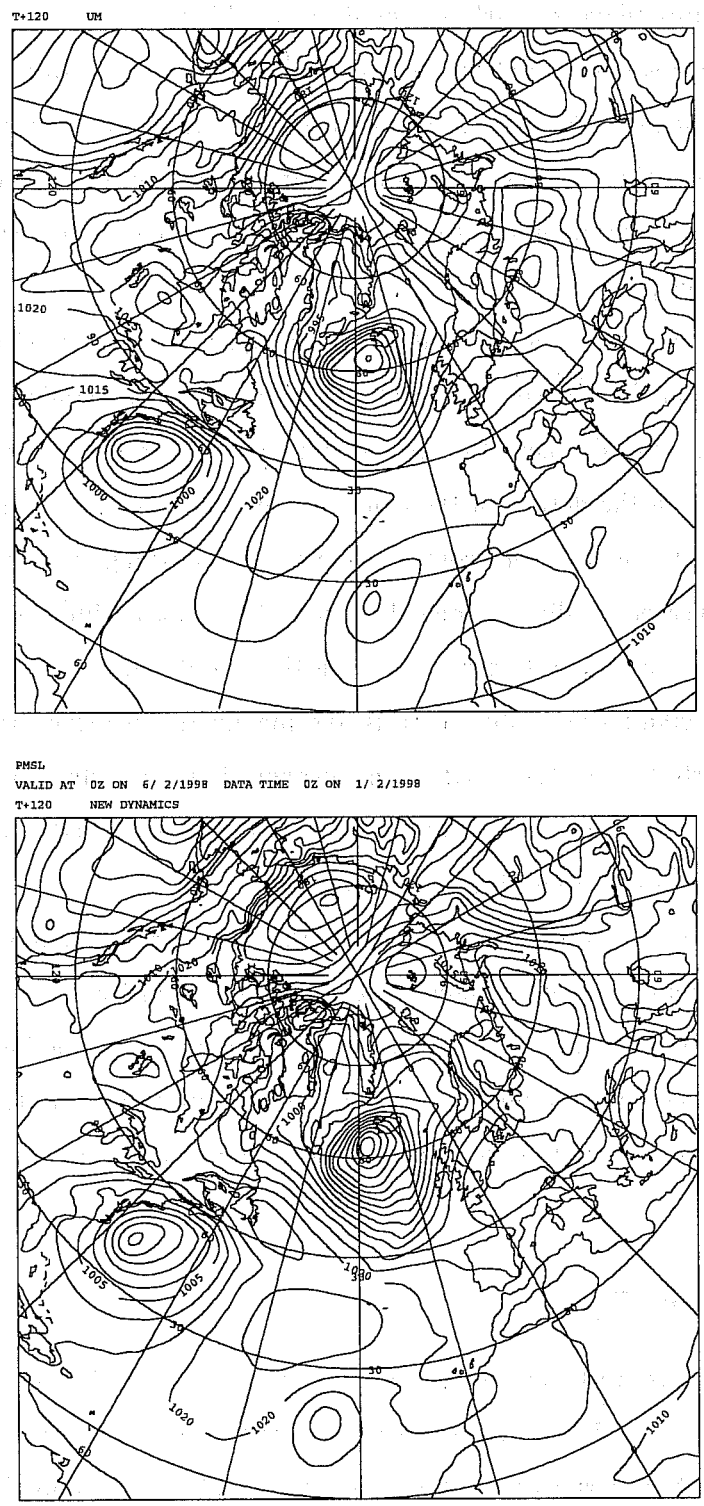

Figure 7: PMSL (5hPa contours) for T+120 forecast valid at 00UTC 6/2/98. Upper panel from UM. Lower panel from new dynamics.

for a profile of temperatures on a set of pressure levels we need to calculate the heights, interpolate either (Exner) pressure or (potential) temperature to new height levels and obtain either (potential) temperature or (Exner) pressure from the hydrostatic equation. We also need to interpolate winds both horizontally from a B-grid to C-grid and vertically from a Lorenz staggering to the Charney-Phillips staggering. The interpolation leads to errors at initial time which only gradually reduce in time relative to the forecast error growth. Nonetheless, results are encouraging on the limited number of cases run so far and error growth rates during the forecasts are similar to that of the UM. For a comparison, figure 7 shows five day forecasts of PMSL for regions bordering the Atlantic Ocean in the Northern hemisphere. Results from the UM are in the upper panel and results from new dynamics are in the lower panel. The forecasts are similar overall but as expected there are differences in detail.

8 Conclusions and Future Plans

By the end of 1998, it is hoped that we have obtained results of sufficient quality to justify building the next version of the UM with the new dynamics during the first half of 1999. We need to be confident that outstanding issues can be resolved satisfactorily during 1999 with operational forecast implementation targeted for the spring 2000. Building into the UM will include coupling to VAR and forecast tests including data assimilation will follow. Building into the UM will also allow coupling with the ocean model for ocean-atmosphere climate testing.

Further issues to be addressed include:

- The use of a fully-interpolating scheme for the vertical advection of potential temperature rather than the non-interpolating scheme used. For the other variables we already use a fully-interpolating scheme.

- A semi-Lagrangian treatment rather than the Eulerian treatment of the continuity equation. In the global model the Eulerian treatment allows formal mass conservation but this means using a third advection scheme in our formulation.

- The approximations made in the treatment of various non-linear terms. Alternative choices may be more accurate and stable at little extra cost.

References

[1] Bates, J.R. Moorthi, S. and Higgins, R.W. (1993). A global multilevel atmospheric model using a vector semi-Lagrangian finite-difference scheme. Part1: Adiabatic formulation. *Mon. Wea. Rev.*, *121*, 244-263.

[2] Cullen, M. J. P. (1989). Implicit finite difference methods for modelling discontinuous atmospheric flows. *J. Comp. Phys.* , *81*, 319-348.

[3] Cullen, M.J.P., Davies, T., Mawson, M.H., James, J.A., and Coulter, S. (1997). An overview of numerical methods for the next generation of NWP and climate models. *Numerical Methods in Atmosphere and Ocean Modelling. The Andre Robert Memorial Volume. (C.Lin, R.Laprise, H.Ritchie, Eds.), Canadian Meteorological and Oceanographic Society, Ottawa, Canada* , 425-444.

[4] Cullen, M. J. P. (1997). New mathematical developments in atmosphere and ocean dynamics, and their application to computer simulations. *NWP Division Scientific Paper No. 48.*

[5] Cullen, M.J.P., Davies, T. and Mawson, M.H. (1997). A semi-implicit integration scheme for the Unified Model. *NWP Division Working Paper No. 154.*

[6] Edwards, J.M., and Slingo, A. (1996). Studies with a flexible new radiation code. Part I. Choosing a configuration for a large-scale model. *Quart. J. Roy. Met. Soc.*, *122*, 689-719.

[7] Golding, B.W. (1992). An efficient non-hydrostatic forecast model. *Meteorol. Atmos. Phys.*, *50*, 89-103.

[8] Golding, B.W. (1993). A study of the influence of terrain on fog development.*Mon. Wea. Rev.*, *121*, 2529-2541.

[9] Held, I.M. and Suarez, M.J. (1994). A proposal for the intercomparison of the dynamical cores of atmospheric general circulation models. *Bull. AMS,75*, 1825-1830.

[10] Malcolm, A.J. (1996). Evaluation of the proposed new Unified Model scheme versus the current Unified Model scheme on the shallow water equations. *NWP Division Technical Report No. 180*

[11] Nakamura, N. and Held, I.M. (1989). Nonlinear equilibration of two-dimensional Eady waves. *J. Atmos. Sci.*, *46*, 3055-3064.

[12] Robert, A. (1993). Bubble convection experiments with a semi-implicit formulation of the Euler Equations. *J. Atmos. Sci.*, *50*, 1865-1873.

[13] Skamarock, W.C., Smolarkiewicz, P.K. and Klemp, J.B. 1996 Preconditioned conjugate-residual solvers for Helmholtz equations in non-hydrostatic models. *Mon. Wea. Rev.*, *125*, 587-599.

[14] Smolarkiewicz, P. K. and Margolin L.G. (1994) .Variational Elliptic Solver for Atmospheric Applications. *Los Alamos Report LA-12712-MS.*

[15] Straka, J.M., Wilhelmson, R.B., Wicker, L.J., Anderson, J.R. and Droegemeier, K.K. (1993). Numerical Solutions of a non-linear density current: A benchmark solution and comparisons. *Int. Jour. Num. Methods in Fluids*, *17*, 1-22.

[16] Williamson, D.L., Drake, P., Hack, J.J., Jakob, R. and Swarztrauber, P.N. (1992) A standard test set for numerical approximations to the shallow water equations in spherical geometry. *Journal Comp. Phys.* , *102*, 211-224.